LA-UR 93-638

LA-UR--93-638

DE93 008735

TITLE: HIGH RESOLUTION SIGNAL SYNTHESIS FOR TIME-FREQUENCY DISTRIBUTION

AUTHOR(S): Gregory S. Cunningham and William J. Williams

SUBMITTED TO: INT'L CONF. OF ACOUSTICS, SPEECH AND SIGNAL PROCESSING
'93 ICASSP IEEE CONFERENCE
MINNEAPOLIS
APRIL 27-30, 1993

Los Alamos

Los Alamos National Laboratory
Los Alamos, New Mexico 87545

HIGH-RESOLUTION SIGNAL SYNTHESIS FOR TIME-FREQUENCY DISTRIBUTIONS

Gregory S. Cunningham[1] *and William J. Williams* [2]

[1] Los Alamos National Laboratory, MS P912, Los Alamos, NM 87544
e-mail: cunning@rho.lanl.gov

[2] EECS Department, University of Michigan, Ann Arbor, MI 48109
e-mail: wjw@hippy.eecs.umich.edu

ABSTRACT

Bilinear time-frequency distributions (TFDs) offer improved resolution over linear time-frequency representations (TFRs), but many TFDs are costly to evaluate and are not associated with signal synthesis algorithms. Recently, the spectrogram (SP) decomposition and weighted reversal correlator decomposition have been used to define low-cost, high-resolution TFDs. In this paper, we show that the vector-valued "square-root" of a TFD (VVTFR) provides a representational underpinning for the TFD. By synthesizing signals from modified VVTFRs, we define high-resolution signal synthesis algorithms associated with TFDs. The signal analysis and synthesis packages can be implemented as weighted sums of SP/short-time Fourier Transform signal analysis and synthesis packages, which are widely available, allowing the interested non-specialist easy access to high-resolution methods.

1. BACKGROUND

First, we restate the SP decomposition and weighted reversal correlator decomposition (WRCD). Discrete-time TFDs can be defined in an inner product form [1, 3, 7],

$$C_x(n,\omega;\psi) = <\tilde{\psi} S_{-n} M_{-\omega} x, S_{-n} M_{-\omega} x> \qquad (1)$$

where $\tilde{\psi}$ is the self adjoint linear operator associated with the real valued TFD, and S_{-n} and $M_{-\omega}$ are time and frequency shift operators, respectively. The spectral representation of $\tilde{\psi}$ ($\tilde{\psi}$ is compact if the kernel is square integrable)

$$\tilde{\psi} = \sum_k \lambda_k P_k \qquad (2)$$

where P_k is the projection onto the eigenfunction, e_k, yields the TFD as a weighted sum of SPs,

$$\begin{aligned} C_x(n,\omega;\psi) &= \sum_k \lambda_k \| P_k S_{-n} M_{-\omega} x \|^2 \\ &= \sum_k \lambda_k \left| \sum_{n'} x(n+n') e_k^*(n') e^{-j\omega(n+n')} \right|^2 \end{aligned}$$

This research was supported in part by the Office of Naval Research, ONR contract no. N00014-90-J-1654, and the National Science Foundation, NSF grant no. BCS 9110571

The eigenvalues of $\tilde{\psi}$, $\{\lambda_k\}$, are non-negative if and only if the associated TFD is non-negative [2].

For an arbitrary non-negative TFD, the associated VVTFR is defined as the vector-valued square root of the TFD's inner product form:

$$\begin{aligned} V_x(n,\omega;\psi) &= M_\omega S_n \tilde{\psi}^{\frac{1}{2}} S_{-n} M_{-\omega} x \\ &= \sum_k \lambda_k^{\frac{1}{2}} <x, M_\omega S_n e_k> M_\omega S_n e_k \end{aligned}$$

and can be interpreted as the "local" signal at each time-frequency sample (n,ω). The relationship between the short-time Fourier Transform (STFT) and SP,

$$\begin{aligned} SP_x(n,\omega;w) &= |S_x(n,\omega;w)|^2 \\ &= \| <x, M_\omega S_n w> M_\omega S_n w \|^2, \end{aligned}$$

where $w(n)$ is the SP/STFT analysis window, is easily extended to other non-negative TFDs and their associated VVTFRs:

$$C_x(n,\omega;\psi) = \| V_x(n,\omega,\psi) \|^2 \qquad (3)$$

The polar form of $\tilde{\psi}$ is $\tilde{\psi} = UP$, where U is unitary (all of its eigenvalues have magnitude one) and P is positive (all of its eigenvalues are non-negative). Under mild support and window constraints [2], U is the reversal operator for many high resolution TFDs, yielding the WRCD for high resolution TFDs [3]:

$$C_x(n,\omega;\psi) = WD_{V_x(n,\omega,\psi)}(n,\omega) \qquad (4)$$

where

$$V_x(n,\omega,\psi) = M_\omega S_n P^{\frac{1}{2}} S_{-n} M_{-\omega} x \qquad (5)$$

is a local representation of the signal underlying the TFD and $WD_x(n,\omega)$ is the discrete time Wigner distribution (DTWD) of $x(n)$.

Note that the difference between non negative TFDs and high resolution TFDs is the unitary operator used to map the local signal onto a positive or real value. Both low resolution TFDs and high resolution TFDs admit a representation of the signal using time frequency localized functions.

However, for the DTWD, the local representation of the signal is just the signal itself: $V_x(n,\omega,\psi_{WD}) = x$ for all n,ω.

where ψ_{WD} is the WD kernel. Shenoy and Parks also note that the WD is non-representational [7]. They contend that the WD is more properly regarded as a tool for specifying and interpreting time-varying filters (signal synthesis algorithms) than as a signal transformation itself. They use the Weyl correspondence to visualize time-varying filters in the time-frequency domain. The Weyl correspondence associates a time-frequency mask, $M(n, \omega)$, to the linear operator (time-varying filter/signal synthesis algorithm), L, via

$$< Lx, x > = \sum_n \int M(n, \omega) WD_x(n, \omega) d\omega \qquad (6)$$

Hlawatsch [5] also implicitly uses the Weyl correspondence for defining time-varying filters using time-frequency domain descriptions.

2. HIGH-RESOLUTION SIGNAL SYNTHESIS

Least-squares signal synthesis from modified VVTFRs associated with non-negative TFDs can be proposed,

$$\hat{x} = \arg\min_x \sum_n \int \| V_x(n, \omega; \psi) - M(n, \omega) V_x(n, \omega; \psi) \|^2 d\omega \qquad (7)$$

and solved as the weighted sum of solutions to least-squares signal synthesis from modified STFTs:

$$\hat{x} = \frac{1}{\sum_k \lambda_k} \sum_k \lambda_k \hat{x}_k \qquad (8)$$

where

$$\hat{x}_k = \arg\min_x \sum_n \int | S_x(n, \omega; e_k) - M(n, \omega) S_x(n, \omega; e_k) |^2 d\omega \qquad (9)$$

is the least-squares solution to a signal synthesis problem from a modified STFT (see Figure 1).

The signal synthesis algorithm in (8)-(9) can be generalized to high-resolution TFDs, where $\hat{x}_k$ is still given by (9) and $\{\lambda_k\}$ and $\{e_k\}$ are the eigenvalues and eigenfunctions of ψ, as in (2). Some of the eigenvalues will be negative, since the TFD is no longer non-negative.

Note that, because some of the eigenvalues are negative, the high resolution algorithm is not the least-squares solution to a modified VVTFR problem as in (7). However, some of the properties of the algorithm illustrate that it may be a very useful tool regardless.

For example, if the TFD satisfies time and frequency marginal properties, then $M(n, \omega) = m(n)$ yields $\hat{x}(n) = m(n)x(n)$ and $M(n, \omega) = M(\omega)$ yields $\hat{x}(n) = m(n) *_n x(n)$, where $M(\omega)$ is the discrete time Fourier Transform of $m(n)$. The Weyl correspondence demonstrates the same "marginal properties" [7] because the kernel for the WD satisfies the time and frequency marginal properties.

Finally, if $M(n, \omega) = \delta(n - n_o, \omega - \omega_o)$, then

$$[illegible] \qquad (10)$$

Alternatively, a synthesized signal that might better correspond to this particular mask is the local signal, x $V_x(n, \omega; \psi)$. The local signal may be useful for non-parametrized detection/estimation and other problems [2].

The signal synthesis algorithms in (8)-(9) are all linear maps of the original signal, $\hat{x} = L(\psi, M)x$. The character of the linear map, L, depends on the associated TFD kernel, ψ, and the mask, $M(n, \omega)$. We can write a "correspondence rule" for linear maps associated with a particular TFD kernel:

$$< L(\psi, M)x, x > = \sum_n \int M(n, \omega) C_x(n, \omega; \psi) d\omega \qquad (11)$$

Since $C_x(n, \omega, \psi)$ is just a smoothed version of the DTWD, the equivalent mask, $\tilde{M}(n, \omega)$ which yields the linear map, $L(\psi, M)$, via the Weyl correspondence in (6) is just a smoothed version of $M(n, \omega)$ [2]. The interpretation of this is that signal synthesis associated with a TFD other than the WD gives you worse time-frequency resolution than implied by $M(n, \omega)$.

The degree to which $M(n, \omega)$ is smeared to yield $\tilde{M}(n, \omega)$ is dictated by the time-frequency spread of the TFD kernel. For the SP, $M(n, \omega)$ is smoothed by the WD of the SP window, which will have time-frequency spread approximately equal to or greater than a Heisenberg cell. Higher resolution TFDs have kernels which have much less spread than the SP kernel.

The smoothing of $M(n, \omega)$ has been noted elsewhere for the case of signal synthesis from modified short-time Fourier Transforms [7] and more general signal synthesis algorithms [6]. Smearing of $M(n, \omega)$ can allow undesired noise or components to "bleed in" to the desired synthesized signal, as we illustrate with several examples in the next section.

3. EXAMPLES

In Figure 2 we demonstrate the effect of smearing and the utility of the local signal. Figure 2a contains the SP of a 64-point complex tone embedded in complex, white gaussian noise of equal total energy using a 64-point rectangular window, and Figure 2d contains the Binomial distribution [8] of the same signal. Figures 2b and 2e contain the real part of the local signals for each of the two TFDs at the time frequency center of the complex tone, and Figures 2c and 2f contain the DTWDs of the signals synthesized from each of the two TFDs using a 0/1 mask whose rectangular boundary is superimposed on all of the greyscale TFDs. Note that all of the DTWDs in Figure 2 are plotted only for frequencies in the range $[-\frac{\pi}{2}, \frac{\pi}{2}]$ since the DTWD is periodic in π, hence the mask boundaries appear twice as tall as they do in the other TFDs.

The DTWD of the signal synthesized from the Binomial distribution (Fig. 2f) is as good as that from the matched window SP (Fig. 2c). Also, the local signal for the Binomial distribution (Fig. 2e) properly identifies the locally tonal nature of the signal. The local signal for the SP (Fig. 2b) can only be a time frequency translate of the window function, which is the noise free complex tone in this case.

Figure 2g contains the SP of a narrow gaussian transient embedded in complex, white gaussian noise of equal total energy using a 64 point rectangular window, and Figure

2j contains the Binomial distribution of the same signal. Figures 2h and 2k contain the real part of the local signals for each of the two TFDs at the time-frequency center of the transient, and Figures 2i and 2l contain the DTWDs of the signals synthesized from each of the two TFDs using a 0/1 mask whose rectangular boundary is superimposed on all of the greyscale TFDs.

This time, the DTWD of the signal synthesized from the Binomial distribution (Fig. 2l) is much better than that from the badly mismatched SP (Fig. 2i). The local signal for the Binomial distribution (Fig. 2k) properly identifies the locally transient nature of the signal, while the local signal for the SP (Fig. 2h), which is again a time-frequency translate of the window function, is a very poor representation of the locally transient nature of the signal.

4. CONCLUSION

We have discussed high-resolution signal synthesis algorithms which can be implemented as weighted sums of STFT synthesis algorithms. The high-resolution algorithms were derived as an extension of least-squares signal synthesis from modified time-frequency indexed local signals, which provide a representational underpinning for the associated TFD. The algorithms exhibit desirable properties, relate easily to the Weyl correspondence and yield results superior to STFT signal synthesis for a simple example.

If there are only a few significant terms in the SP decomposition of a high-resolution TFD, then the associated signal synthesis algorithm defined in (8)-(9) can be approximately implemented using only a few STFT signal synthesis units. In previous work, we have used the SP decomposition to define fast approximations to desirable high resolution TFDs [4] when the SP decomposition yields only a few significant terms.

The results in this paper along with our previous work define a high-resolution signal analysis and synthesis package which can be implemented using only a few weighted SP/STFT signal analysis and synthesis units (Figure 1). Experimenters who have access to SP/STFT packages can now easily gain access to high resolution analysis and synthesis packages through simple modifications to their existing software.

5. REFERENCES

[1] M.G. Amin, "Performance Comparison of Wigner-Ville Spectrum Estimators using Least Squares Approximation of Kernels," *Proc. ISSPA*, Gold Coast, Australia, vol. 2, 1990.

[2] G.C. Cunningham, "Analysis, Synthesis and Implementation of Time-Frequency Distributions using the SP decomposition," Ph.D. dissertation, University of Michigan, 199[illegible].

[3] G.C. Cunningham and W.J. Williams, "Decomposition of Time-Frequency Distribution Kernels," to appear in *Advanced Signal Processing Algorithms, Architectures and Implementations III, SPIE Proceedings vol. 1770*, San Diego, CA, July 19-25, 1992.

[4] G.C. Cunningham and W.J. Williams, "Fast Implementations of Time-Frequency Distributions," *IEEE-SP Intl. Symp. Time-Frequency and Time-Scale Analysis*, Victoria, British Columbia, pp. 241-244, October 4-6, 1992.

[5] F. Hlawatsch, W. Kozek, and W. Krattenthaler, "Time-Frequency Subspaces and their Application to Time-Varying Filtering," *ICASSP-90*, Albuquerque, NM, pp. 1607-1610.

[6] W. Kozek, "On the Generalized Weyl Correspondence and its Application to Time-Frequency Analysis of Linear Time-Varying Systems," *IEEE-SP Intl. Symp. Time-Frequency and Time-Scale Analysis*, Victoria, British Columbia, pp. 167-170, October 4-6, 1992.

[7] R.G. Shenoy and T.W. Parks, "The Weyl Correspondence and Time-Frequency Analysis," submitted to *IEEE Trans. Signal Proc.*, in March 1991, revised April 1992.

[8] W.J. Williams and J. Jeong, "Reduced Interference Time-Frequency Distributions," Chapter 3 of *Time-frequency Analysis and Its Applications*, ed. B. Boashash, Longman and Cheshire, 1992.

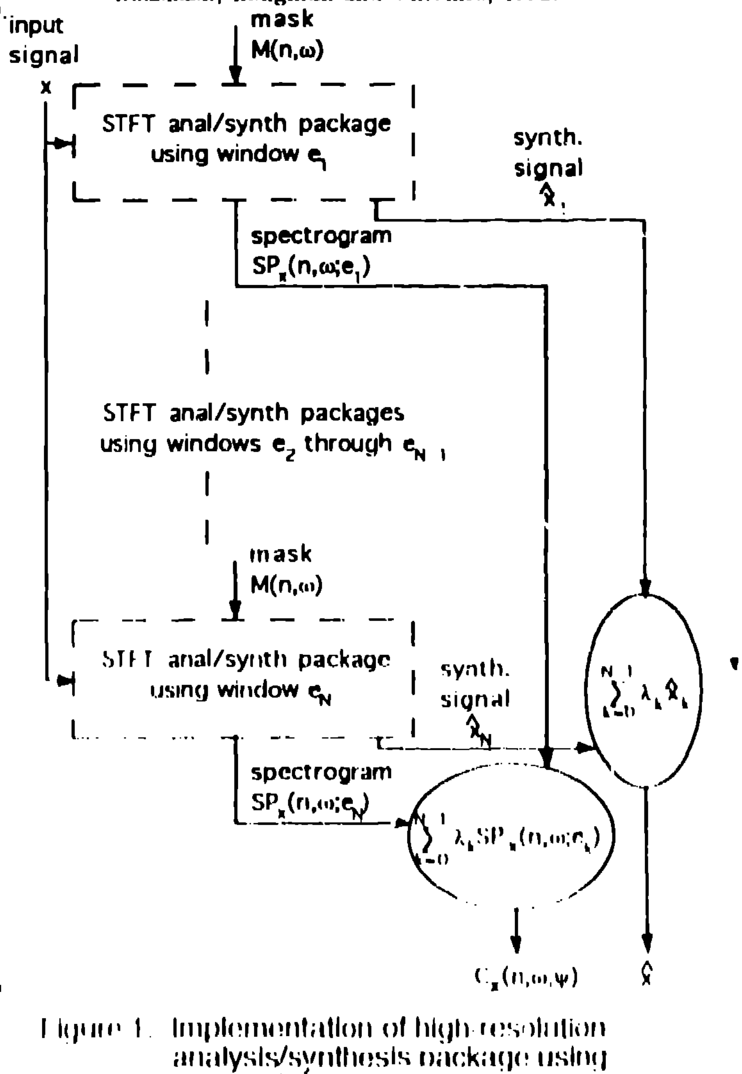

Figure 1. Implementation of high-resolution analysis/synthesis package using SPs and STFTs.

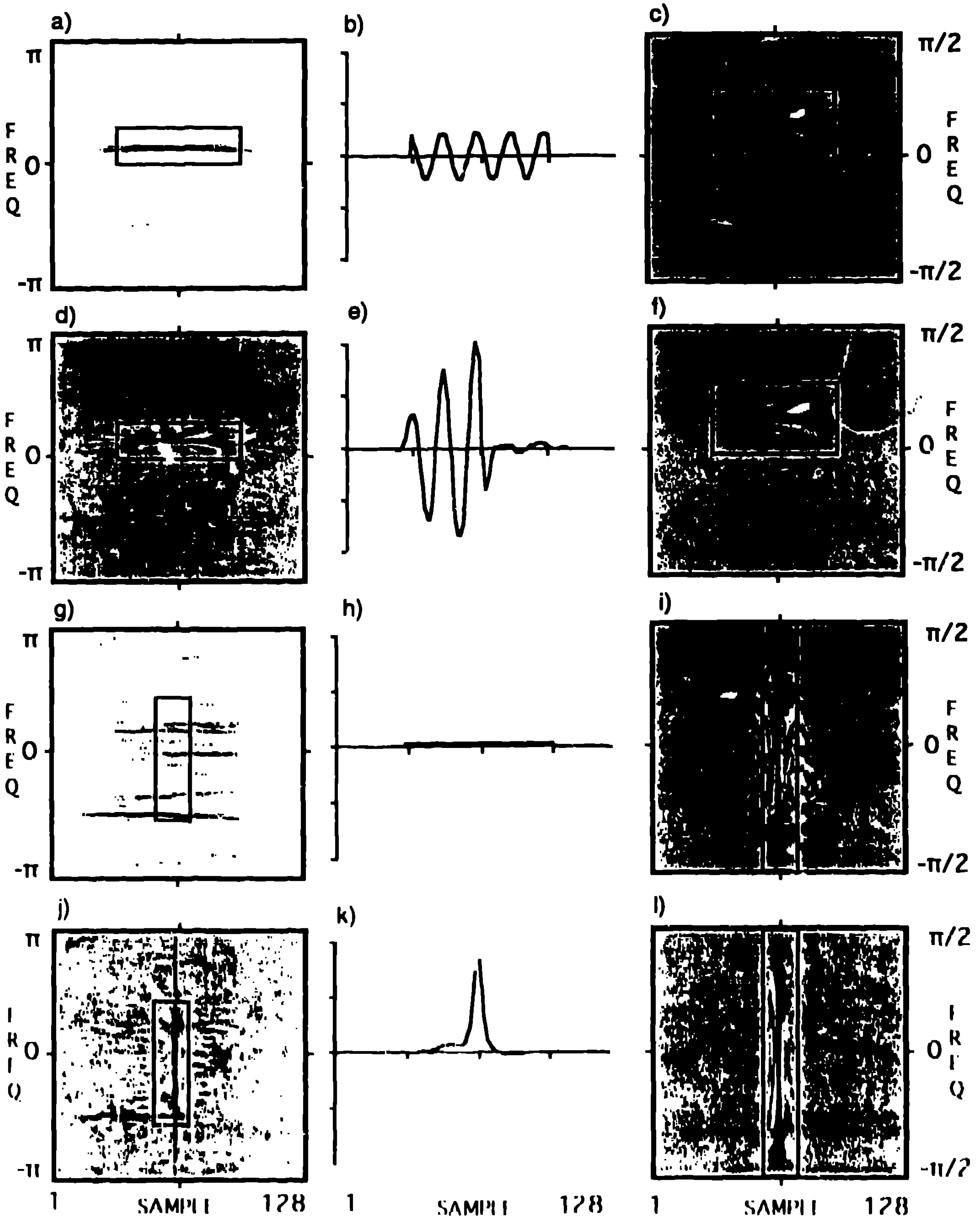

Figure 2 Example of the smearing of the desired time-frequency mask and the utility of the local signal